Published in final edited form as:
Opt Lett. 2013 May 1; 38(9): 1515–1517.

Flexible endoscope for continuous *in vivo* multispectral fluorescence lifetime imaging

Shuna Cheng[1], **J. Jesus Rico-Jimenez**[1], **Joey Jabbour**[1], **Bilal Malik**[1], **Kristen C. Maitland**[1], **John Wright**[2], **Yi-Shing Lisa Cheng**[2], and **Javier A. Jo**[1,*]

[1]Department of Biomedical Engineering, Texas A&M University, Emerging Technologies Building, College Station, TX 77843, USA

[2]Department of Diagnostic Sciences, Texas A&M University Health Science Center – Baylor College of Dentistry, 3302 Gaston Avenue, Dallas, TX 75246, USA

Abstract

Fluorescence lifetime imaging (FLIM) offers a noninvasive approach for characterizing the biochemical composition of biological tissue. There has been an increasing interest in the application of multispectral FLIM for medical diagnosis. Central to the clinical translation of FLIM technology is the development of compact and high-speed endoscopy systems. Unfortunately, the predominant multispectral FLIM approaches suffer from limitations that impede the development of endoscopy systems that are suitable for *in vivo* tissue imaging. We present a compact wide-field time-gated FLIM flexible endoscope capable of continuous lifetime imaging of up to three fluorescence emission bands simultaneously. This novel endoscope design will facilitate the evaluation of FLIM for *in vivo* applications.

In recent years, there has been an increasing interest in evaluating the application of endogenous Fluorescence Lifetime Imaging (FLIM) for clinical diagnosis. A central issue for the clinical translation of FLIM is the development of compact and fast FLIM endoscopy systems suitable for *in vivo* tissue imaging. However, the FLIM endoscope designs proposed thus far, including those summarized below, are still not well suited for clinical applications.

In FLIM, the fluorescence lifetime is measured at each spatially resolvable location within a fluorescence image. The fluorescence lifetime can be measured in the frequency domain by estimating the phase shift or amplitude modulation in a fluorescence signal obtained by modulated excitation of the sample.[1] Alternatively, the fluorescence lifetime can be measured in the time domain by directly measuring the fluorescence decay after a pulse excitation, using time-gated imaging for wide-field FLIM, or either time-correlated single-photon counting (TCSPC) or the direct pulse recording implementation in point scanning systems.[1]

Several FLIM endoscope designs have already been proposed. Two wide-field FLIM rigid endoscope designs were proposed, one in the frequency-domain[2] and the other in the time-domain.[3, 4] Although these two designs allowed video-rate FLIM imaging, they were limited to a single emission band, and illumination was delivered through an optical path external to the endoscope. Two flexible endoscope designs have been proposed using a scanning FLIM implementation based on TCSPC.[5, 6] However, these designs were also limited to a single

*Corresponding author: javierjo@tamu.edu.

emission band and to visible wavelength excitation, restricting their use to exogenous fluorescence imaging.

To the best of our knowledge, Elson et al. reported the first and only multispectral FLIM flexible endoscope design, based on a wide-field time-gating FLIM implementation.[7] The endoscope was built around a flexible imaging fiber bundle, multispectral imaging was realized by placing a filter wheel in the emission optical path, and illumination was delivered using an adjacent multimode fiber. This endoscope was recently used to image oral cancer and brain cancer *in vivo*.[8, 9] Although the results of these two pilot studies were promising, this design presented two main limitations. First, since multispectral imaging is sequential, the time required to record FLIM images at multiple emission bands increases with the number of spectral bands.[8, 9] Second, since illumination light is delivered through a fiber adjacent to the imaging bundle, achieving uniform illumination and endoscope compactness can be challenging.

To overcome these limitations, we have designed a flexible FLIM endoscope capable of simultaneous multispectral FLIM imaging at an acquisition speed of ~2 fps. The schematic of the proposed system is shown in Fig. 1. Since tissue endogenous fluorescence is best excited with UV light, a frequency-tripled Q-switched Nd:YAG laser was used as the excitation source (355nm, <1ns pulse width, maximum repetition rate of 100 kHz, AOT-YVO-100QSP/MOPA, Advanced Optical Technology, UK). The endoscope was built around an imaging fiber bundle suitable for UV-VIS light transmission (10,000 elements, NA of 0.22, 1.1mm active area diameter, bending radius of 200 mm, 1 m long, FIGR-10, Fujikura). A Lithium-based GRIN lens (NA of 0.20, 1 mm diameter, GRINTECH GmbH) cemented at the distal end of the bundle provides a working distance of 5 mm and a field of view of 2.25 mm in diameter (2.25× magnification). A dichroic mirror (DM1: T>95%@380–800nm, Chroma), placed at the proximal end of the imaging bundle, was used to reflect the laser beam into the fiber bundle and transmit the fluorescence emission to the detection arm. The laser beam size was allowed to be slightly larger than the bundle active area to achieve uniform illumination at the cost of coupling efficiency (~35%).

Wide-field time-gated FLIM was implemented using an intensified charge-coupled device or ICCD camera (200–800 nm spectral range, 14.4 × 10.8 mm^2 active area, 780 × 580 pixels, minimum gate time of 200 ps, 33.8 Hz frame rate, 4Picos, Stanford Computer Optics). Simultaneous multispectral FLIM was implemented as follows, based on a similar approach previously proposed by Siegel.[10] The fluorescence emission exiting the proximal end of fiber bundle was first collimated by an achromatic lens (L1: 35 mm focal length). Then, a combination of two dichroic mirrors and one reflective mirror (DM2: T>95% @ 439–647nm, DM3: T>95% @ 492–950nm, M1: Ravg> 97.5% @ 450–2000 nm) with three band pass filters (F2: 390±20 nm, F3: 450±20 nm, F4: 560±20 nm) were used to separate the fluorescence emission into three spectrally resolved collimated beams. Each beam was then directed and focused on different regions of the ICCD active area by means of three reflective mirrors (M2: Ravg >90% from 250 – 450 nm, M3–4: Ravg>97.5%@450–2000 nm) and an achromatic lens (L2: 150 mm focal length). The three spectral channels were selected based on the peak emission of three fluorophores of interest (collagen, NADH and FAD, respectively); however, they can be customized as needed.

In the presented configuration, the spatial resolution of the system was limited by the fiber bundle core-to-core spacing, not the pixel size of the active area of the ICCD. The sample was imaged onto the distal end of the fiber bundle with demagnification of ~2.25x. Therefore, the ~12 μm core-to-core spacing of the fiber bundle corresponds to a ~27 μm spot separation in the sample. The proximal end of the imaging bundle was imaged onto the ICCD with a magnification of ~4.3×, resulting in ~52 μm separation between individual

fibers in the ICCD image plane, compared to the ICCD pixel size of 18 μm. Thus, in this configuration, subdividing the active area of the ICCD to accommodate multiple spectral images did not decrease the imaging spatial resolution, which was ultimately limited by the fiber bundle core-to-core spacing. The measured lateral resolution in all three spectral channels was estimated to be ~35 μm by imaging a USAF resolution target (NT57-895, Edmund Optics).

The fluorescence lifetime maps were calculated using the rapid lifetime determination (RLD) algorithm, which requires only two time-gated fluorescence images recorded at different delays with respect to the excitation pulse.[11] The width for both gates was set up at about half of the expected lifetime of the sample. The first gate was temporally placed right after the fluorescence peak emission. The second gate was placed immediately after the end of the first gate (without overlapping). The RLD algorithm treats the fluorescence decays as single exponentials, which is seldom the case for tissue autofluorescence; nevertheless, the approximated average lifetime can still provide fluorescence lifetime contrast in biological samples.[3, 4] The implementation of this algorithm in our wide-field FLIM system allowed an imaging speed of ~2 fps. For all experiments, the laser repetition rate was set to 10 kHz, the pulse energy at ~0.8 uJ, and the integration time per gate was set to 20 ms, resulting in sufficient SNR. Although in principle it should be possible to attain a FLIM acquisition speed equal to half the frame rate of the ICCD (33.8 Hz), the time required to change the time-gated image delay at each consecutive frame is still too long (~250 ms) with the current ICCD control software. We are currently modifying the ICCD drivers to reduce this time and achieve higher imaging speed.

The FLIM endoscope was first validated with a set of three quartz capillary tubes loaded with 1 mM solutions of POPOP (in ethanol), NADH and FAD (both in PBS). The fluorescence intensity and average lifetime images from the three spectral channels are displayed in Fig. 2. Strong emission from POPOP was observed in both the 390±20 nm and 450±20 nm bands, while NADH and FAD emission was only observed in the 450±20 nm and 560±20 nm bands, respectively. The observed average lifetime for POPOP, NADH, and FAD were 1.07±0.24 ns, 0.51±0.06 ns, and 2.32±0.56 ns, respectively (calculated pixel-to-pixel for the areas corresponding to the entire capillary). The results from the three FLIM channels were in good agreement with the emission spectra and lifetimes of the three fluorophores.[12]

The FLIM endoscope was further validated by imaging *in vivo* a lesion from a hamster check pouch that was diagnosed by histopathology as dysplasia. The imaging protocol was approved by the Institutional Animal Care and Use Committee at Texas A&M University. Multispectral FLIM images of the oral lesion surrounded by healthy tissue are displayed in Fig. 3. The fluorescence intensity images showed stronger fluorescence in the surrounding healthy tissue relative to the lesion area for all spectral channels. The fluorescence lifetime images for the 390±20 nm and 450±20 nm channels showed longer values in the surrounding healthy tissue (~2–3 ns) relative to the lesion area (~1.2–1.6 ns). The fluorescence lifetime image for the 560±20 nm channel showed longer values in the lesion area (~1.6–1.7ns) relative to the surrounding healthy tissue (~1.2–1.3 ns). These fluorescence intensity and lifetime values resemble both NADH and FAD emission in the lesion area, and collagen emission in the surrounding healthy tissue. These results are also consistent with the biochemical composition of normal and cancerous epithelial tissue.[8, 12]

Taking advantage of the relatively fast acquisition speed (~2 fps), we also demonstrated continuous multispectral FLIM imaging. First, two quartz capillary tubes loaded with 1 mM solutions of POPOP (in ethanol) and NADH (in PBS) were continuously imaged. A total of ten consecutive fluorescence intensity and lifetime frames for the 450±20 nm channel are

shown in Media-1. The lifetime maps clearly show longer lifetimes for the POPOP capillary (bottom) compared to the NADH capillary (top). To investigate the robustness of the imaging system to movement artifacts, the position of the capillaries was shifted by the 6th frame. While the intensity maps were not affected, the lifetime values were underestimated for part of the POPOP capillary during the shift in the capillary position; however, the lifetime map was stabilized after one frame as expected, since only two consecutive gated images are required to estimate a lifetime image.

Continuous multispectral FLIM imaging was also demonstrated *in vivo* on the same hamster cheek pouch lesion of Fig. 3. A total of ten consecutive fluorescence intensity and lifetime frames for the three spectral channels are shown in Media-2. The contrast in both fluorescence intensity and lifetime for the three spectral channels was maintained throughout the whole imaging sequence.

In summary, we have presented a small-diameter FLIM flexible endoscopy system based on a coherent optical fiber bundle suitable for both UV excitation and UV-Vis collection that is capable of continuous lifetime imaging of up to three fluorescence emission bands simultaneously. This novel endoscope design will facilitate the evaluation of multispectral endogenous FLIM for *in vivo* applications.

Supplementary Material

Refer to Web version on PubMed Central for supplementary material.

Acknowledgments

This work was supported by the National Institutes of Health (R01 CA138653, R01 HL11136).

References

1. Lakowicz JR. (Springer, New York. 2006
2. Mizeret J, Stepinac T, Hansroul M, Studzinski A, van den Bergh H, Wagnieres G. Review of Scientific Instruments. 1999; 70(12):4689–4701.
3. Munro I, McGinty J, Galletly N, Requejo-Isidro J, Lanigan PMP, Elson DS, Dunsby C, Neil MAA, Lever MJ, Stamp GWH, French PMW. Journal of Biomedical Optics. 2005; 10(5)
4. Requejo-Isidro J, McGinty J, Munro I, Elson DS, Galletly NP, Lever MJ, Neil MAA, Stamp GWH, French PMW, Kellett PA, Hares JD, Dymoke-Bradshaw AKL. Optics Letters. 2004; 29(19):2249–2251. [PubMed: 15524370]
5. Kennedy GT, Manning HB, Elson DS, Neil MAA, Stamp GW, Viellerobe B, Lacombe F, Dunsby C, French PMW. J Biophotonics. 2010; 3(1–2):103–107. [PubMed: 19787682]
6. Fruhwirth GO, Ameer-Beg S, Cook R, Watson T, Ng T, Festy F. Opt Express. 2010; 18(11):11148–11158. [PubMed: 20588974]
7. Elson DS, Jo JA, Marcu L. New Journal of Physics. 2007; 9:127. [PubMed: 19503759]
8. Sun Y, Phipps J, Elson DS, Stoy H, Tinling S, Meier J, Poirier B, Chuang FS, Farwell DG, Marcu L. Opt Lett. 2009; 34(13):2081–2083. [PubMed: 19572006]
9. Sun YH, Hatami N, Yee M, Phipps J, Elson DS, Gorin F, Schrot RJ, Marcu L. Journal of Biomedical Optics. 2010; 15(5)
10. Siegel J, Elson DS, Webb SED, Parsons- Karavassilis D, Leveque-Fort S, Cole MJ, Lever MJ, French PMW, Neil MAA, Juskaitis R, Sucharov LO, Wilson T. Optics Letters. 2001; 26(17): 1338–1340. [PubMed: 18049601]
11. Agronskaia AV, Tertoolen L, Gerritsen HC. J Phys D Appl Phys. 2003; 36(14):1655–1662.
12. Shrestha S, Applegate BE, Park J, Xiao X, Pande P, Jo JA. Opt Lett. 2010; 35(15):2558–2560. [PubMed: 20680057]

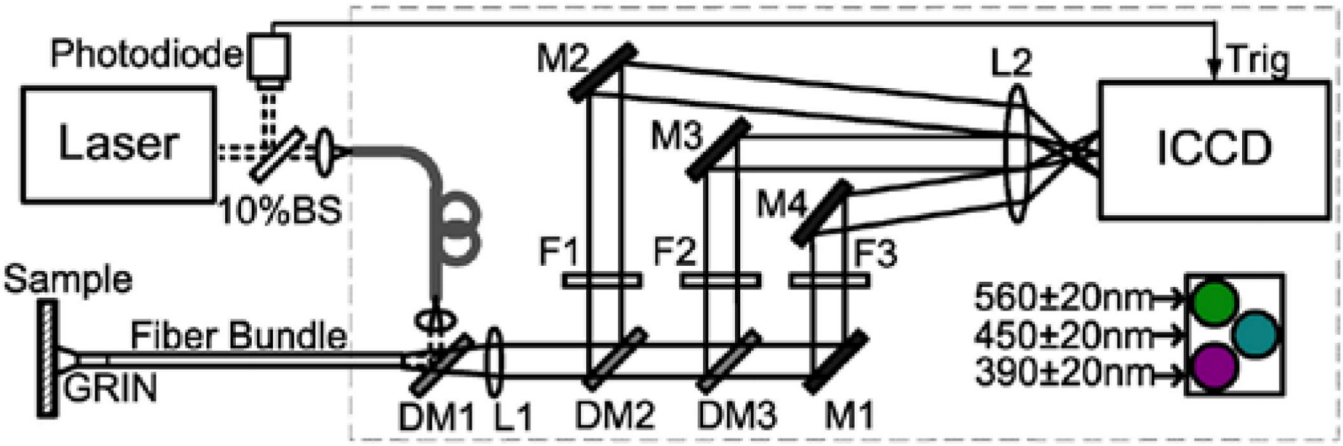

Fig. 1.
Schematic of the FLIM endoscopy system. BS-Beam sampler, DM-Dichroic mirror, M-Mirror, F-Filter, L-Lens.

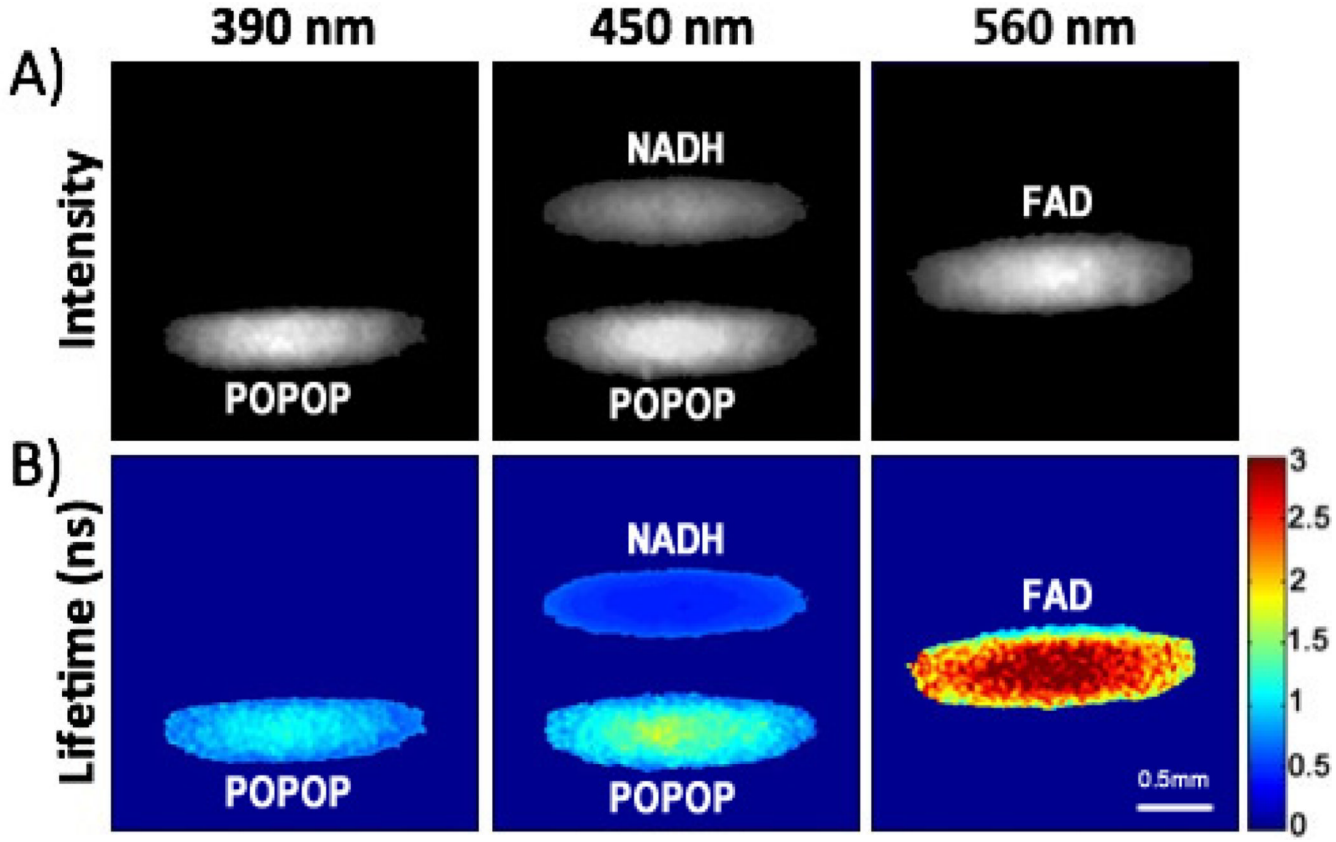

Fig. 2.

In vitro validation imaging of quartz capillaries loaded with (top to bottom) NADH, FAD, and POPOP: (A) fluorescence intensity maps (B) lifetime maps (colorscale in ns). Continuous imaging of two capillaries loaded with POPOP and NADH was also demonstrated (Media-1, 450±20 nm channel only).

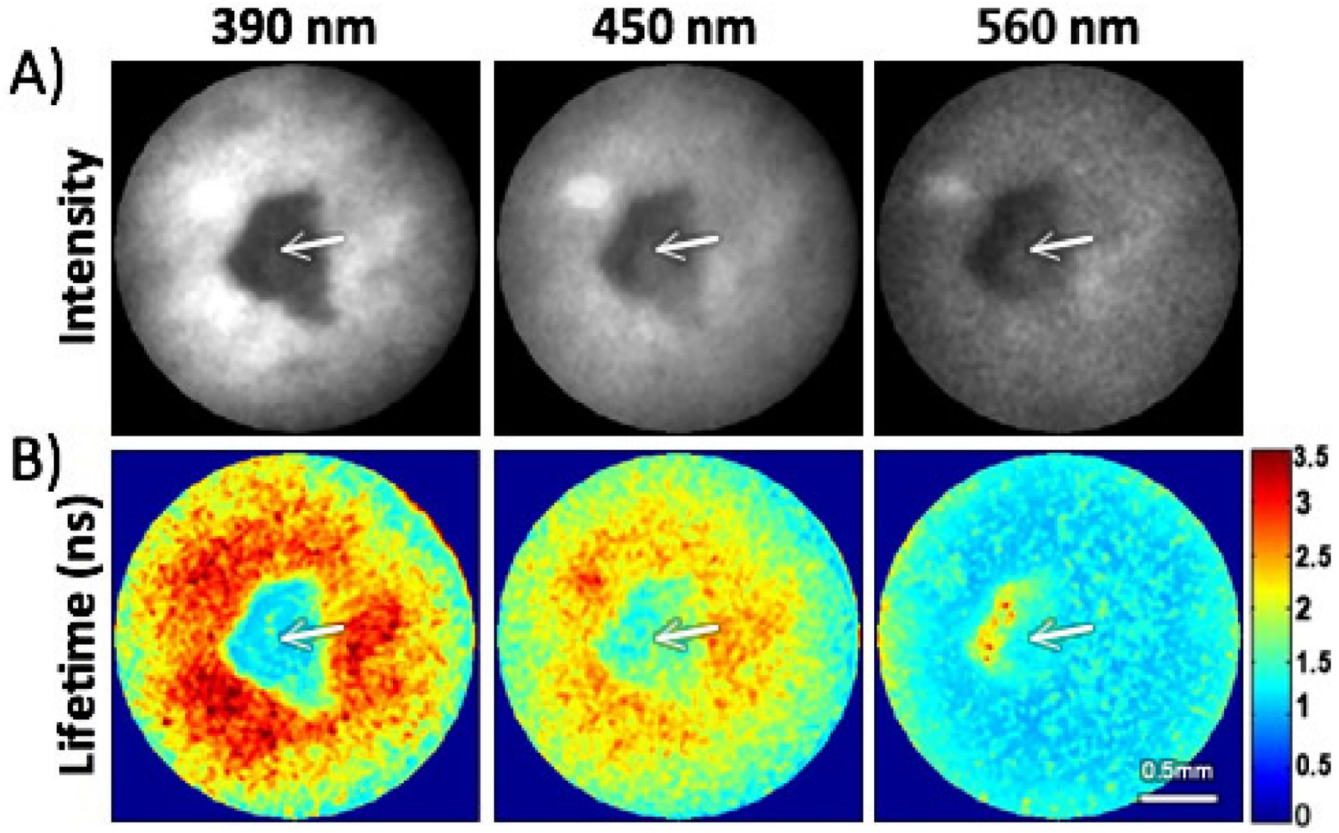

Fig. 3.

In-vivo validation imaging of a hamster cheek pouch: (A) fluorescence intensity maps (B) lifetime maps (colorscale in ns). The arrows indicate a small malignant lesion showing distinct fluorescence intensity and lifetime values than those from the surrounding tissue. Continuous in-vivo imaging of the same lesion was also demonstrated (Media-2).